Surface-Assisted Laser Desorption/Ionization of Trinitrotoluene on Porous Silicon under Ambient Conditions

ARTICLE *in* THE JOURNAL OF PHYSICAL CHEMISTRY C · FEBRUARY 2015

Impact Factor: 4.77 · DOI: 10.1021/jp5129063

5 AUTHORS, INCLUDING:

Igor' L. Martynov
National Research Nuclear University MEPHI
22 PUBLICATIONS **70** CITATIONS
SEE PROFILE

Dmitriy Dovzhenko
National Research Nuclear University MEPHI
7 PUBLICATIONS **4** CITATIONS
SEE PROFILE

THE JOURNAL OF PHYSICAL CHEMISTRY C

Article

pubs.acs.org/JPCC

Surface-Assisted Laser Desorption/Ionization of Trinitrotoluene on Porous Silicon under Ambient Conditions

Yury Kuzishchin, Igor Martynov,* Dmitriy Dovzhenko, Gennadii Kotkovskii, and Alexander Chistyakov

Department of Physics of Micro- and Nanosystems, National Research Nuclear University MEPhI (Moscow Engineering Physics Institute), 31 Kashirskoe sh., 115409 Moscow, Russian Federation

Supporting Information

ABSTRACT: Desorption/ionization on silicon (DIOS) is widely used in modern mass spectrometry for obtaining ions of various organic substances. The high efficiency of DIOS suggests that it may be a promising method in ion-mobility spectrometry (IMS) using gas-phase ion separation. The influence of laser wavelength and intensity on DIOS of trinitrotoluene (TNT) molecules under ambient conditions has been studied. If laser with a wavelength of 266 or 355 nm is used, TNT molecules predominantly form $(TNT - H)^-$ negative ions. Their formation has been found to result from laser-induced proton transfer from TNT molecules to the porous silicon (pSi) surface, rather than gas-phase ion−molecule reactions. The dependence of the yield of $(TNT - H)^-$ ions on the laser intensity has been analyzed. The ion yield curve has been demonstrated to fit the Arrhenius function at laser intensity lower than $\sim 2.5 \times 10^7$ W/cm^2. Experiments have shown that the desorption/ionization of TNT molecules is not a purely thermal process. The results demonstrate that DIOS can be widely used in the IMS technology.

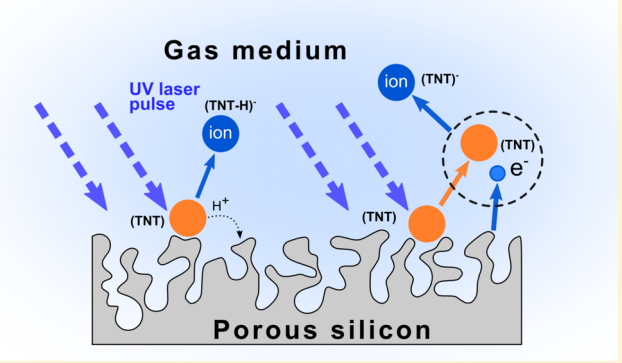

1. INTRODUCTION

Detection of small amounts of organic compounds is a topical problem. It is of special importance in the field of safety and security provision, specifically for detecting toxicants, drugs, and explosives. A wide range of methodologies, including optical spectroscopy,[1−4] mass spectrometry (MS),[5] and chromatography,[6] is used in this area. Ion-mobility spectrometry (IMS) stands out from the other approaches due to its unique combination of a high sensitivity, unrivaled quickness of analysis, and the possibility of compact instrumental embodiment. State-of-the-art IMS instruments have a detection threshold of about 10^{-13} to 10^{-14} g/cm^3 with a weight of 3−6 kg and an analysis time of less than 10 s.[7,8]

The IMS approach is based on analysis of the spectrum of ion drift in a gas or gas mixture in a constant electric field.[9] The type of analyzed ion is characterized by its mobility[9] (k) defined as the ratio of the ion drift velocity to the electric field intensity.

At present, numerous ionization methods are used to obtain the ions of the analyte. Of special interest is desorption/ionization on silicon (DIOS),[10−16] which is a special case of surface-assisted laser desorption/ionization (SALDI)[17−22] and is similar to the well-known matrix-assisted laser desorption/ionization (MALDI) method.[23−25] The DIOS method is effective in analysis of low-molecular-weight compounds (lighter than 600 Da) due to the absence of the background signal from the matrix.[11,12,26,27] This, together with the high adsorption capacity of porous silicon (pSi) due to its large specific surface area, makes DIOS a promising method to be used in IMS. Study of the mechanisms of ion formation is an important task of its own, because the gas medium may substantially influence them. The results of preliminary studies suggest that laser-induced electron emission from the pSi surface, which initiates various gas-phase ion−molecule reactions,[28,29] plays a role in the ion formation. These processes may substantially complicate the resultant ion spectrum.[30]

The purpose of this study was to analyze the formation of negative ions induced by laser irradiation of the pSi chip with 2,4,6,-trinitrotoluene (TNT) molecules adsorbed on it under ambient conditions.

We chose the nitroaromatic compound TNT because it is one of the most widely used explosives, which makes the detection of its traces an important problem.

2. EXPERIMENTAL METHODS

Figure 1 shows a schematic diagram of the experimental setup. Its basis is an ion mobility spectrometer of original design described in detail elsewhere.[28] The drift-tube length of the spectrometer is 18.5 cm, which, at an electric field intensity of 200 V/cm, ensures a resolution of 70.[31] The ion current was detected using a Faraday plate detector containing an electrometric amplifier with a current−voltage conversion factor of $\sim 10^{10}$ V/A.

A 2 × 2 mm pSi chip was mounted on a metal rod in the ion source perpendicularly to the laser beam. The rod allowed the

Received: December 26, 2014
Revised: February 21, 2015
Published: February 23, 2015

DOI: 10.1021/jp5129063
J. Phys. Chem. C 2015, 119, 6382−6388

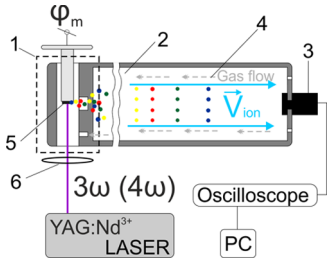

Figure 1. Schematic diagram of the experimental setup: 1, ion source; 2, drift-tube; 3, detector; 4, buffer gas flow; 5, pSi wafer; and 6, quartz lens.

position of the pSi chip relative to the spectrometer axis to be adjusted. For effective ejection of ions, ejection voltage was applied to the pSi chip.[28]

The nonionized part of the analyte was prevented from entering the drift-tube of the spectrometer by a buffer gas flow in the direction opposite to that of the ion movement. The buffer gas was either air purified by means of a 4A molecular sieve or pure nitrogen.

The pSi chip was irradiated using the third (3ω) and fourth (4ω) harmonics of a YAG:Nd^{3+} laser. The laser operated in the Q-switched mode. Laser pulses repetition rate was 10 Hz with 6 ns duration. The intensity distribution in the beam cross section corresponded to the TEM_{00} mode. The laser pulse fluence (F) on the pSi chip varied from 15 to 300 mJ/cm^2, which corresponded to intensities (q) from 2.5×10^6 to 5.0×10^7 W/cm^2.

pSi substrates were obtained by electrochemical etching of the monocrystalline silicon wafer with aqueous solution of hydrofluoric acid. We used n-type silicon with a resistivity of 0.01 Ω cm and the (111) orientation. An aqueous solution of hydrofluoric acid with a HF to H_2O ratio of 1:5 served as an electrolyte. The etching was performed for 10 min at a current density of 10 mA/cm^2. The samples were illuminated with a halogen lamp during the etching.

Figure 2 shows typical scanning electron microscopy (SEM) images of the surface and a cross section of a pSi substrate. The image has been obtained using an RAITH 150 TWO scanning electron microscope. As can be seen in the figure, the porous layer was ~20 μm in thickness. The pores of the substrate obtained had a hierarchical structure, which is typical of macroporous silicon obtained using an aqueous solution of hydrofluoric acid as an electrolyte and n-type silicon wafers.[32] For example, the SEM images showed that there were structures with a characteristic size of ~1 μm on the pSi surface. On the other hand, the samples exhibited photoluminescence in the range of 500−700 nm upon UV excitation, which indicated that their crystal structure contained pores with a characteristic size smaller than 10 nm.[33]

The analyte was applied onto the pSi chip by adsorbing its vapors from a gas phase. In contrast to adsorption from a solution, this method precludes the influence of solvent molecules on desorption/ionization.

The device for adsorption was an airtight glass cuvette containing a pSi chip and a source of TNT in the form of a film applied onto glass. The cuvette could be heated for controlling the pressure of saturated TNT vapors. The gas phase temperature was monitored using a thermocouple.

Depending on the experimental conditions, the adsorption was performed either in air atmosphere or in the atmosphere of pure nitrogen. The typical time of TNT vapor adsorption was 10 min at a temperature of 55 °C. In the case of the nitrogen atmosphere, the residual oxygen concentration in the cuvette was monitored using an oxygen sensor; it was no higher than 0.1 vol %. If necessary, excess oxygen was removed from pores by placing the pSi chip into a nitrogen atmosphere for 30 min at 100 °C.[34] According to published data,[35,36] these conditions ensure the elimination of oxygen molecules from pSi pores. After the adsorption, the pSi chip was withdrawn from the cuvette, mounted on a rod, and introduced into the ion source of the spectrometer. The pSi chip was exposed to air for no longer than 1 min. After the chip was introduced into the ion source, it was additionally flushed with nitrogen for 5 min to remove the possible contamination before the measurements started.

The amount of TNT adsorbed on the surface of the pSi chip under these conditions was estimated to be no greater than 100 ng/cm^2, which is much less than the weight of a monolayer. This allowed us to be certain that most TNT molecules directly contacted pSi, the contribution of direct absorption of radiation by TNT molecules themselves to the heating of the surface being minor.

3. RESULTS AND DISCUSSION

Nitroaromatic compounds are traditionally detected using the negative mode of IMS (detection of negative ions) because of a lower background signal and higher amplitude of the useful signal.[37−41]

3.1. Background Signal. The behavior of the so-called background IMS spectrum is an important factor that should be taken into account in the analysis of the results. It is formed upon laser irradiation of the pSi chip in a gas medium in the absence of adsorbed molecules of the analyte.

In the negative-ion mode, the background IMS spectrum (Figure 3), irrespective of the excitation wavelength, is mainly accounted for by ions of the same type, $O_2^-\bullet(H_2O)_n$, with the reduced mobility[9] k_0 = 2.19 cm^2/V s.[28,42] Ions of this type are formed when oxygen molecules capture free electrons during

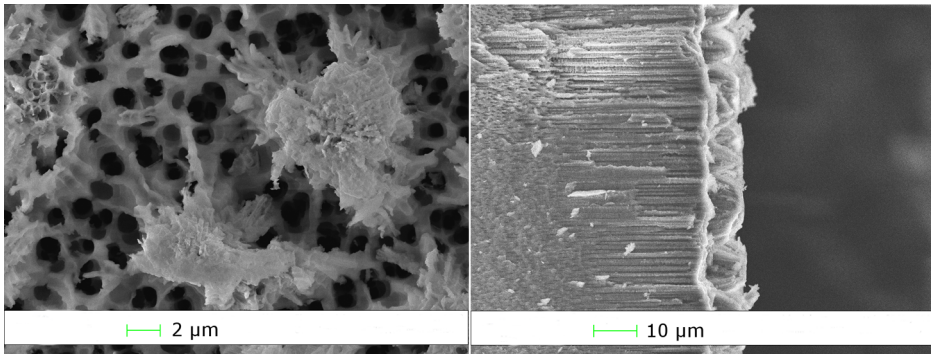

Figure 2. SEM images of the surface (left) and a cross section (right) of a typical pSi substrate.

DOI: 10.1021/jp5129063
J. Phys. Chem. C 2015, 119, 6382−6388

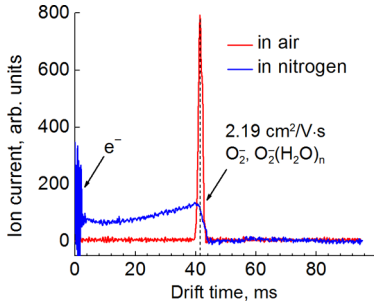

Figure 3. Negative-ion mode background IMS spectra induced by UV laser irradiation of a pSi chip. The characteristic prolonged signal in the case of nitrogen corresponds to molecular oxygen ions formed through the capture of free electrons by residual oxygen in the drift tube of the spectrometer.[39,43−45]

ionization by almost any method. In the case of laser irradiation of the pSi chip, this results from laser-induced electron emission.[28]

This can be demonstrated experimentally by replacing air with nitrogen as a buffer gas. Indeed, in the nitrogen atmosphere, the ion peak amplitude with k_0 = 2.19 cm^2/V s drops by more than an order of magnitude, the peak itself is characteristically prolonged,[39,43−45] and a signal corresponding to free electrons appears at the beginning of the sweep[39,43−45] (Figure 3). This unambiguously indicates that the negative-ion mode background IMS spectrum is only formed in the gas phase, due to electron emission and ion−molecule reactions.[39,43−45]

3.2. DIOS Ion Mobility Spectra of TNT. In experiments where purified air was used as a buffer gas, UV laser irradiation ($q \approx 1.5 \times 10^7$ W/cm^2) of the pSi chip with TNT molecules adsorbed on it resulted in an additional ion peak in the negative-ion spectrum. The reduced mobility of the detected ions was 1.55 cm^2/V s, irrespective of the radiation wavelength (λ = 266 or λ = 355 nm). Ions with this reduced mobility are well-known and are identified as $(TNT - H)^-$.[38] Typical DIOS IMS spectrum of TNT at λ = 266 nm is shown in Figure 4.

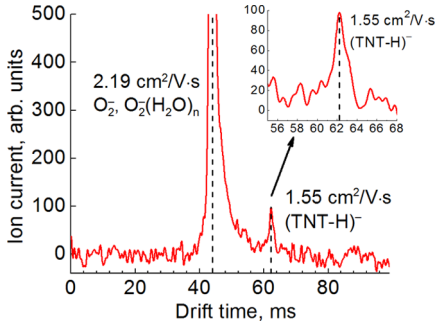

Figure 4. DIOS IMS spectrum of negative ion of TNT in air for laser wavelength λ = 266 nm.

The mechanism of the formation of $(TNT - H)^-$ ions remains an open question. These ions may result from gas-phase ion−molecule reactions between desorbed TNT molecules, electrons emitted from the pSi chip upon laser irradiation, and air oxygen.[38,39] The characteristic reactions involved in this mechanism are well-known:[38,39]

$$O_2 + e^- \rightarrow O_2^-$$

$$TNT + O_2^- \rightarrow [TNT{\bullet}O_2]^- \rightarrow (TNT - H)^- + HO_2$$

Note that the formation of $(TNT - H)^-$ ions in gas-phase ion−molecule reactions is the prevailing mechanism if laser irradiation of the pSi chip is used for ionizing TNT vapors.[28] On the other hand, $(TNT - H)^-$ ions may result from proton transfer processes on the pSi chip surface.[15,46]

Since the efficiency of gas-phase TNT molecules deprotonation critically depends on the oxygen concentration,[28,38,39] mechanism of the formation of $(TNT - H)^-$ can be determined from experiments with changing the gas medium of the spectrometer from air to pure nitrogen and removing residual oxygen from pSi pores. The results of these experiments are shown in Figure 5.

As can be seen in Figure 5, the amplitude of the $(TNT - H)^-$ signal was decreased less than 20% after the change of the gas medium, irrespective of the radiation wavelength. Therefore, the efficiency of $(TNT - H)^-$ ion formation is practically independent of the oxygen concentration; hence, these ions are formed directly on the pSi chip surface.

In this case, proton transfer to the pSi chip surface is the most probable mechanism of the ion formation. Indeed, since there are broken bonds on the sample surface, formation of Si−H bonds is energetically favorable (75 kcal/mol) and, hence, highly probable.

Note also that the IMS spectra in nitrogen contain, in addition to the peak of $(TNT - H)^-$ ions, a peak with k_0 = 1.49 cm^2/V s corresponding to TNT^- ions.[38,39] It is probably accounted for by the small part of TNT molecules that leave the surface in the neutral state and are ionized in the gas phase by directly capturing electrons emitted from the pSi chip surface.[38,39] This would be the only peak in the case of domination of TNT molecules gas-phase ionization.

3.3. Dependence of the $(TNT - H)^-$ Signal Amplitude on the Laser Radiation Intensity. Figure 6 shows the dependences of the amplitude of the $(TNT - H)^-$ ion signal on the laser pulse intensity and fluence.

Each of these dependences can be divided into two regions: region I where the ion signal amplitude rises and region II where it declines. The ion signal degradation (region II) started when the laser intensity (q) exceeded ~2.5 × 10^7 W/cm^2 [or laser fluence (F) exceeded ~150 mJ/cm^2]. SEM data demonstrated intense thermal destruction of the pSi ship surface upon laser irradiation in region II (Figure 7). Exposure to laser irradiation with $q < 2 \times 10^7$ W/cm^2 (F < 120 mJ/cm^2) (region I) did not cause noticeable alteration of the surface. These results agree with the published data.[14]

The ion signal amplitude increased with an increase in laser intensity in region I. At a constant q, the signal was stable and remained unchanged after exposure of the pSi chip to as many as 500 laser pulses. The maximum ion signal amplitude for laser wavelength λ = 266 nm was an order of magnitude higher compared to λ = 355 nm (Figure 6).

There is no consensus about the mechanism of ion formation during DIOS. However, most researchers agree that localization of excited carriers in surface trap states followed by thermal desorption of analyte molecules plays an important role in the formation of positive ions of the $(MH)^+$ type.[16,47] Both processes are related to heating the pSi chip surface by laser irradiation and can be described by the Arrhenius equation for the yield of ions with the activation energy E_d:

$$I \sim \exp(-E_d/k_B T) \quad (1)$$

Apparently, as in the case described in refs 16 and 47, the formation of $(TNT - H)^-$ negative ions is related to the heating of the pSi chip surface by laser irradiation. Therefore, it is reasonable to use the same Arrhenius equation for analyzing the

DOI: 10.1021/jp5129063
J. Phys. Chem. C 2015, 119, 6382−6388

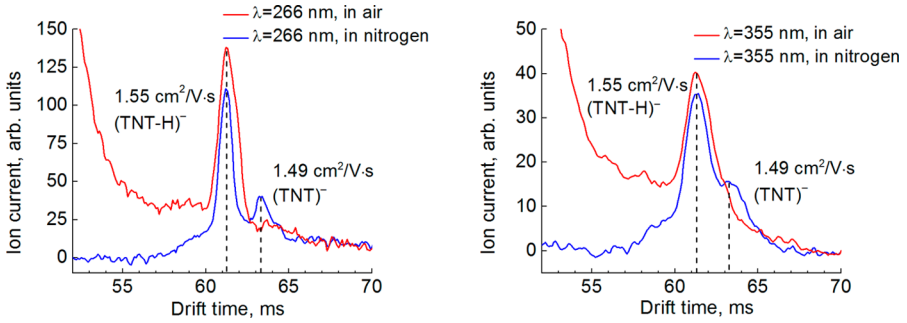

Figure 5. DIOS IMS spectra of negative ions of TNT in different gas media at laser wavelengths λ = 266 nm (left) and λ = 355 nm (right).

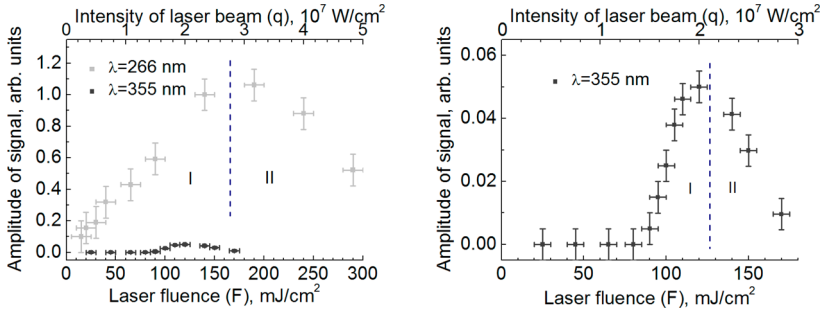

Figure 6. Left: dependence of the amplitude of the $(TNT - H)^-$ ion signal on laser pulse intensity and fluence for wavelengths λ = 266 nm and λ = 355 nm. Right: The dependence for λ = 355 nm shown to a larger scale. The measurements were performed in air.

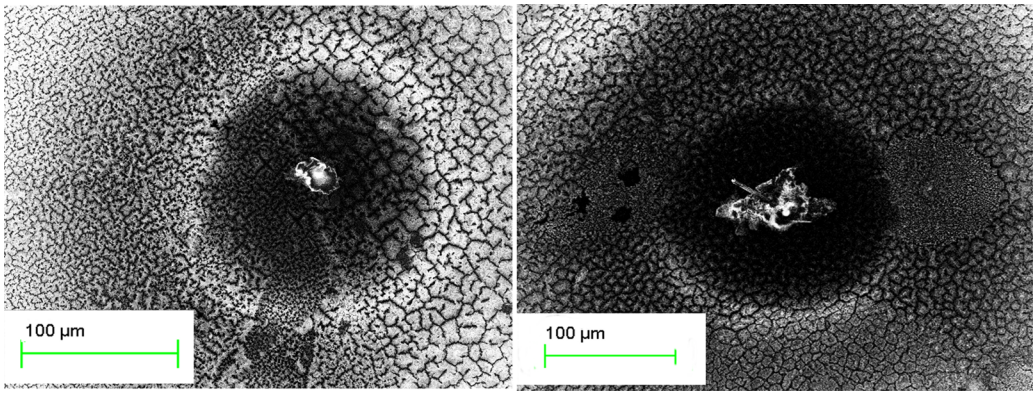

Figure 7. SEM images of pSi chip surface exposed to 100 laser pulses with $q \approx 4.5 \times 10^7$ W/cm^2 ($F \approx 250$ mJ/cm^2) for wavelengths λ = 266 nm (left) and λ = 355 nm (right).

dependece of the $(TNT - H)^-$ signal amplitude on the laser pulse intensity.

Since the characteristic depth of penetration of laser pulses with λ = 266 nm and λ = 355 nm into pSi ($1/\alpha$, where α is the absorption coefficient) is an order of magnitude smaller than the heat diffusion length during the time of laser pulse action (l_d) (Table 1),

Table 1. Optical and Thermodynamic Characteristics of pSi at λ = 266 nm and λ = 355 nm

laser radiation wavelength, λ (nm)	266	355
heat conductivity coefficient, χ (W/m K) at T = 300 K	~50[48,49]	
volume heat capacity, C_v (J/K cm^3) at T = 300 K	0.7[50,51]	
time of laser irradiation, τ (ns)	6	6
depth of heat diffusion, l_d (cm), $\{2[\tau(\chi/C_v)]^{1/2}\}$	10^{-4}	10^{-4}
absorption coefficient, α (cm^{-1})	4×10^5[52]	2×10^5[52]
reflectance, R	~0.3	~0.3

the dependence of the pSi chip surface temperature on the laser fluence (F) can be written as

$$T = \eta F + T_0 = \frac{(1 - R)}{C_v l_d} F + T_0 \quad (2)$$

where T_0 is the initial pSi chip temperature (in K), C_v is the volume heat capacity of pSi (in J/K cm^3), and R is the pSi reflectance.

Estimation of the coefficient η from the data shown in Table 1 yields the same value $\eta \approx 10$ K cm^3/mJ for laser wavelength λ = 266 nm and λ = 355 nm.

A more detailed approach to the calculation of η requires that the dependences of the volume heat capacity, C_v, heat conductivity, χ, and, hence, heat diffusion depth, l_d, on temperature be taken into account. The product $C_v l_d$ for bulk silicon has been reported[53,54] to decrease by about half with an

DOI: 10.1021/jp5129063
J. Phys. Chem. C 2015, 119, 6382−6388

increase in temperature from 300 to 1000 K. However, as follows from other data,[48,49] this effect for pSi should be weaker and can be neglected in our study.

The results of approximation of the experimental data for region I by eq 2 are presented in Figure 8, which shows the

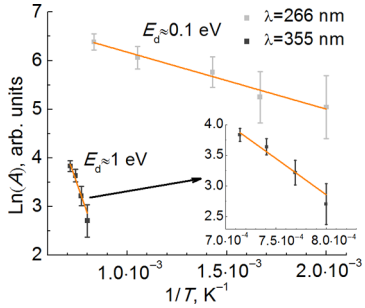

Figure 8. Dependence of the logarithm of the $(TNT - H)^-$ peak amplitude on pSi surface temperature for laser wavelengths $\lambda = 266$ nm and $\lambda = 355$ nm.

dependence of the logarithm of the $(TNT - H)^-$ signal amplitude on the reciprocal temperature (in K^{-1}). As can be seen in the figure, a linear approximation fits the data well, which allows us to use it for estimating the activation energy of the formation of $(TNT - H)^-$ ions.

The estimation gives $E_d \approx 0.1$ eV for $\lambda = 266$ nm and $E_d \approx 1$ eV for $\lambda = 355$ nm. Such a substantial difference between the E_d values indicates that the desorption/ionization of TNT molecules is not a purely thermal process (its initial event is not thermal desorption) and E_d increases with increasing laser wavelength. Indeed, control experiment for laser wavelength $\lambda = 532$ nm showed an absence of the $(TNT - H)^-$ ion signal at laser intensities lower than the threshold of the visible pSi destruction ($q \approx 5 \times 10^7$ W/cm^2, $F \approx 300$ mJ/cm^2). Therefore, according to the same estimation E_d for $\lambda = 532$ nm is substantially higher than 2.5 eV.

The dependence of E_d on λ, as well as the decline of the ion signal upon destruction of the pSi surface, shows that precisely laser irradiation causes the proton transfer from TNT molecules to the surface of the substrate. The difference in E_d also explains the difference in the ion signal amplitude for laser wavelengths $\lambda = 266$ nm and $\lambda = 355$ nm.

Note that the dependence of the activation energy on the laser wavelength was earlier observed for a number of positive ions.[16,47] For example, mass spectrometric studies showed that the activation energy increased with increasing excitation wavelength for positive ions of caffeine.[16] There is no conclusive explanation for this finding thus far; however, the authors of the study[16] attributed this effect to localization of excited carriers in surface traps of pSi. A similar phenomenon is likely to play a role in the formation of $(TNT - H)^-$ negative ions. At the same time, it cannot be excluded that direct laser excitation of TNT molecules affects proton transfer. For example, laser irradiations of a TNT molecule at $\lambda = 266$ nm and $\lambda = 355$ nm excite it into different electron states, which may affect the proton transfer probability.

4. CONCLUSIONS

Thus, we have demonstrated that the DIOS method can be used for ionization of TNT under ambient conditions. It has been shown that TNT molecules upon laser irradiation with wavelength $\lambda = 266$ nm and $\lambda = 355$ nm predominantly form $(TNT - H)^-$ ions. Comparison of the results of ionization in different gas media has led to the conclusion that the formation of $(TNT - H)^-$ ions is accounted for by laser-induced proton transfer from TNT to the pSi surface. We have analyzed the dependence of the ion yield on the laser intensity and found a threshold of ion signal degradation, which is closely correlated with the threshold of laser-induced thermal destruction of pSi. The ion yield curve fits the Arrhenius function at a moderate laser intensity. The activation energy of desorption/ionization (E_d) decreases with decreasing laser wavelength, which indicates that desorption/ionization is not a purely thermal process.

The results of our study demonstrate that the DIOS method can be widely used in the IMS technology and provide further insight into the mechanism of formation of negative ions on the pSi surface upon exposure to UV laser irradiation.

■ ASSOCIATED CONTENT

Supporting Information

Estimation of TNT molecules amount adsorbed on the pSi chip during sorption process and DIOS IMS spectra of a negative ion of TNT in air at a laser wavelength of $\lambda = 266$ nm. This material is available free of charge via the Internet at http://pubs.acs.org.

■ AUTHOR INFORMATION

Corresponding Author

*E-mail: ILMartynov@mephi.ru; I.L.Martynov@gmail.com.

Notes

The authors declare no competing financial interest.

■ ACKNOWLEDGMENTS

This study was supported by the Ministry of Education and Science of the Russian Federation, Grants 3.1718.2014/K, and State Task no. 1718.

■ ABBREVIATIONS

MALDI, matrix-assisted laser desorption/ionization; SALDI, surface-assisted laser desorption/ionization; DIOS, desorption/ionization on silicon; MS, mass spectrometry; IMS, ion mobility spectrometry; TNT, trinitrotoluene; pSi, porous silicon; YAG, yttrium aluminum garnet; TEM, transverse electric and magnetic; SEM, scanning electron microscopy; UV, ultraviolet

■ REFERENCES

(1) Martín-Palma, R. J.; Manso, M.; Torres-Costa, V. Optical Biosensors Based on Semiconductor Nanostructures. *Sensors (Basel)* **2009**, *9*, 5149−5172.

(2) Lauerhaas, J. M.; Credo, G. M.; Heinrich, J. L.; Sailor, M. J. Reversible Luminescence Quenching of Porous Si by Solvents. *MRS Proc.* **2011**, *256*, 137.

(3) Canaria, C. A.; Huang, M.; Cho, Y.; Heinrich, J. L.; Lee, L. I.; Shane, M. J.; Smith, R. C.; Sailor, M. J.; Miskelly, G. M. The Effect of Surfactants on the Reactivity and Photophysics of Luminescent Nanocrystalline Porous Silicon. *Adv. Funct. Mater.* **2002**, *12*, 495.

(4) Chan, S.; Kwon, S.; Koo, T.-W.; Lee, L. P.; Berlin, A. A. Surface-Enhanced Raman Scattering of Small Molecules from Silver-Coated Silicon Nanopores. *Adv. Mater.* **2003**, *15*, 1595−1598.

(5) Shanta, S. R.; Kim, T. Y.; Hong, J. H.; Lee, J. H.; Shin, C. Y.; Kim, K.-H.; Kim, Y. H.; Kim, S. K.; Kim, K. P. A New Combination MALDI Matrix for Small Molecule Analysis: Application to Imaging Mass Spectrometry for Drugs and Metabolites. *Analyst* **2012**, *137*, 5757−5762.

(6) Collin, O. L.; Niegel, C.; Derhodes, K. E.; McCord, B. R.; Jackson, G. P. Fast Gas Chromatography of Explosive Compounds Using a

DOI: 10.1021/jp5129063
J. Phys. Chem. C 2015, 119, 6382−6388

Pulsed-Discharge Electron Capture Detector. *J. Forensic Sci.* **2006**, *51*, 815−818.
(7) Kotkovskii, G. E.; Martynov, I. L.; Novikova, V. V.; Chistyakov, A. A. A. A Laser Ion-Mobility Spectrometer. *Instruments Exp. Technol.* **2009**, *52*, 253−259.
(8) Kotkovskii, G. E.; Sychev, A. V.; Tugaenko, A. V.; Chistyakov, a. a. A Laser Spectrometer of Field-Asymmetric Ion Mobility. *Instrum. Exp. Tech.* **2011**, *54*, 256−261.
(9) Cohen, M. J.; Karasek, F. W. Plasma Chromatography: A New Dimension for Gas Chromatography and Mass Spectrometry. *J. Chromatogr. Sci.* **1970**, *8*, 330−337.
(10) Wei, J.; Buriak, J. M.; Siuzdak, G. Desorption−Ionization Mass Spectrometry on Poroussilicon. *Nature* **1999**, *399*, 243−246.
(11) Alimpiev, S.; Nikiforov, S.; Karavanskii, V.; Minton, T.; Sunner, J. On the Mechanism of Laser-Induced Desorption−Ionization of Organic Compounds from Etched Silicon and Carbon Surfaces. *J. Chem. Phys.* **2001**, *115*, 1891.
(12) Shen, Z.; Thomas, J. J.; Averbuj, C.; Broo, K. M.; Engelhard, M.; Crowell, J. E.; Finn, M. G.; Siuzdak, G. Porous Silicon as a Versatile Platform for Laser Desorption/Ionization Mass Spectrometry. *Anal. Chem.* **2001**, *73*, 612−619.
(13) Go, E. P.; Prenni, J. E.; Wei, J.; Jones, A.; Hall, S. C.; Witkowska, H. E.; Shen, Z.; Siuzdak, G. Desorption/ionization on Silicon Time-of-Flight/Time-of-Flight Mass Spectrometry. *Anal. Chem.* **2003**, *75*, 2504−2506.
(14) Northen, T. R.; Woo, H.-K.; Northen, M. T.; Nordström, A.; Uritboonthail, W.; Turner, K. L.; Siuzdak, G. High Surface Area of Porous Silicon Drives Desorption of Intact Molecules. *J. Am. Soc. Mass Spectrom.* **2007**, *18*, 1945−1949.
(15) Budimir, N.; Blais, J.-C.; Fournier, F.; Tabet, J.-C. Desorption/ionization on Porous Silicon Mass Spectrometry (DIOS) of Model Cationized Fatty Acids. *J. Mass Spectrom.* **2007**, *42*, 42−48.
(16) Li, J.; Lipson, R. H. Insights into Desorption Ionization on Silicon (DIOS). *J. Phys. Chem. C* **2013**, *117*, 27114−27119.
(17) Tanaka, K.; Waki, H.; Ido, Y.; Akita, S.; Yoshida, Y. Protein and Polymer Analyses up to Mlz 100 000 by Laser Ionization Time-of-Flight Mass Spectrometry. *Rapid Commun. Mass Spectrom.* **1988**, *2*, 151−153.
(18) Sunner, J.; Dratz, E.; Chen, Y.-C. Graphite Surface-Assisted Laser Desorption/ionization Time-of-Flight Mass Spectrometry of Peptides and Proteins from Liquid Solutions. *Anal. Chem.* **1995**, *67*, 4335−4342.
(19) Berkenkamp, S.; Karas, M.; Hillenkamp, F. Ice as a Matrix for IR-Matrix-Assisted Laser Desorption/ionization: Mass Spectra from a Protein Single Crystal. *Proc. Natl. Acad. Sci. U.S.A.* **1996**, *93*, 7003−7007.
(20) Fleith, C.; Cantel, S.; Subra, G.; Mehdi, A.; Ciccione, J.; Martinez, J.; Enjalbal, C. Laser Desorption Ionization Mass Spectrometry of Peptides on a Hybrid CHCA Organic-Inorganic Matrix. *Analyst* **2014**, *139*, 3748−3754.
(21) Liu, Q.; Xiao, Y.; Pagan-Miranda, C.; Chiu, Y. M.; He, L. Metabolite Imaging Using Matrix-Enhanced Surface-Assisted Laser Desorption/ionization Mass Spectrometry (ME-SALDI-MS). *J. Am. Soc. Mass Spectrom.* **2009**, *20*, 80−88.
(22) Kawasaki, H.; Takahashi, N.; Fujimori, H.; Okumura, K.; Watanabe, T.; Matsumura, C.; Takemine, S.; Nakano, T.; Arakawa, R. Functionalized Pyrolytic Highly Oriented Graphite Polymer Film for Surface-Assisted Laser Desorption/ionization Mass Spectrometry in Environmental Analysis. *Rapid Commun. Mass Spectrom.* **2009**, *23*, 3323−3332.
(23) Karas, M.; Bachmann, D.; Bahr, U.; Hillenkamp, F.; Processes, Z.; V, E. S. P. B.; Miinster, U. Matrix-Assisted Ultraviolet Laser Desorption of Non-Volatile Compounds. *Int. J. Mass Spectrom. Ion Processes* **1987**, *78*, 53−68.
(24) Karas, M.; Hillenkamp, F. Laser Desorption Ionization of Proteins with Molecular Masses Exceeding 10,000 Da. *Anal. Chem.* **1988**, *60*, 2299−2301.
(25) Ko, K. H.; Kwon, C. Il; Park, S. H.; Han, N. Y.; Lee, H. K.; Kim, E. H.; Hahm, K. B. Application of Matrix-Assisted Laser Desorption/Ionization Time-of-Flight Imaging Mass Spectrometry (MALDI-TOF IMS) for Premalignant Gastrointestinal Lesions. *Clinical Endoscopy* **2013**, *46*, 611−619.
(26) Chen, Y.-C.; Wu, J.-Y. Analysis of Small Organics on Planar Silica Surfaces Using Surface-Assisted Laser Desorption/ionization Mass Spectrometry. *Rapid Commun. Mass Spectrom.* **2001**, *15*, 1899−1903.
(27) Shen, Z.; Thomas, J. J.; Siuzdak, G.; Blackledge, R. D. A Case Study on Forensic Polymer Analysis by DIOS-MS: The Suspect Who Gave Us the SLIP. *J. Forensic Sci.* **2004**, *49*, 1028−1035.
(28) Martynov, I. L.; Karavanskii, V. A.; Kotkovskii, G. E.; Kuzishchin, Y. a.; Tsybin, a. S.; Chistyakov, a. a. Ion Mobility Spectrometer with Ion Source Based on Laser-Irradiated Porous Silicon. *Tech. Phys. Lett.* **2011**, *37*, 15−18.
(29) Dovzhenko, D. S.; Kuzishchin, Y. A.; Martynov, I. L.; Eremin, I. S.; Kotkovskiĭ, G. E.; Chistyakov, A. A.; Krasovskiĭ, V. I.; Sipaĭlo, I. P. The Mechanism of Laser-Stimulated Desorption/ionization of Nitro-aromatic Compounds from a Nanoporous Silicon Surface at Atmospheric Pressure. *J. Opt. Technol.* **2014**, *81*, 435.
(30) Kotkovskii, G. E.; Tugaenko, A. V.; Chistyakov, a. a. Negative Ion Formation in Laser Ion Mobility Increment Spectrometer. *Tech. Phys. Lett.* **2010**, *36*, 276−278.
(31) Revercomb, H. E.; Mason, E. a. Theory of Plasma Chromatography/gaseous Electrophoresis. Review. *Anal. Chem.* **1975**, *47*, 970−983.
(32) Sailor, M. J. *Porous Silicon in Practice*; Wiley-VCH: Weinheim, Germany, 2011.
(33) Cullis, A. G.; Canham, L. T.; Calcott, P. D. J. The Structural and Luminescence Properties of Porous Silicon. *J. Appl. Phys.* **1997**, *82*, 909.
(34) Ott, N.; Nerding, M.; Müller, G.; Brendel, R.; Strunk, H. P. Structural Changes in Porous Silicon during Annealing. *Phys. Status Solidi* **2003**, *197*, 93−97.
(35) Green, S.; Kathirgamanathan, P. The Quenching of Porous Silicon Photoluminescence by Gaseous Oxygen. *Thin Solid Films* **2000**, *374*, 98−102.
(36) Cisneros, R.; Pfeiffer, H.; Wang, C. Oxygen Absorption in Free-Standing Porous Silicon: A Structural, Optical and Kinetic Analysis. *Nanoscale Res. Lett.* **2010**, *5*, 686−691.
(37) Lee, J.; Park, S.; Cho, S. G.; Goh, E. M.; Lee, S.; Koh, S.-S.; Kim, J. Analysis of Explosives Using Corona Discharge Ionization Combined with Ion Mobility Spectrometry-Mass Spectrometry. *Talanta* **2014**, *120*, 64−70.
(38) Ewing, R. G.; Atkinson, D. A.; Eiceman, G. A.; Ewing, G. J. A Critical Review of Ion Mobility Spectrometry for the Detection of Explosives and Explosive Related Compounds. *Talanta* **2001**, *54*, 515−529.
(39) Daum, K. A.; Atkinson, D. A.; Ewing, R. G. The Role of Oxygen in the Formation of TNT Product Ions in Ion Mobility Spectrometry. *Int. J. Mass Spectrom.* **2002**, *214*, 257−267.
(40) Asbury, G. R.; Klasmeier, J.; Hill, H. H. Analysis of Explosives Using Electrospray Ionization/ion Mobility Spectrometry (ESI/IMS). *Talanta* **2000**, *50*, 1291−1298.
(41) Spangler, G. E.; Lawless, P. a. Ionization of Nitrotoluene Compounds in Negative Ion Plasma Chromatography. *Anal. Chem.* **1978**, *50*, 884−892.
(42) Sabo, M.; Matúška, J.; Matejčík, S. Specific O_2^- Generation in Corona Discharge for Ion Mobility Spectrometry. *Talanta* **2011**, *85*, 400−405.
(43) Su, D.; Niu, W.; Liu, S.; Shen, C.; Huang, C.; Wang, H.; Jiang, H.; Chu, Y. Electron Attachment Rate Constant Measurement by Photoemission Electron Attachment Ion Mobility Spectrometry (PE-EA-IMS). *Radiat. Phys. Chem.* **2012**, *81*, 1869−1873.
(44) Kučera, M.; Stano, M.; Wnorowska, J.; Barszczewska, W.; Loffhagen, D.; Matejčík, Š. Electron Attachment to Oxygen in Nitrogen Buffer Gas at Atmospheric Pressure. *Eur. Phys. J. D* **2013**, *67*, 234.
(45) Veber, A. A.; Kotkovskii, G. E.; Martynov, I. L.; Chistyakov, A. A. Formation of Anions of Nitroaromatic Compounds in Gases during UV Laser Irradiation. *Russ. J. Phys. Chem. B* **2010**, *4*, 548−556.
(46) Budimir, N.; Blais, J.-C.; Fournier, F.; Tabet, J.-C. The Use of Desorption/Ionization on Porous Silicon Mass Spectrometry for the Detection of Negative Ions for Fatty Acids. *Rapid Commun. Mass Spectrom.* **2006**, *20*, 680−684.

DOI: 10.1021/jp5129063
J. Phys. Chem. C 2015, 119, 6382−6388

(47) Alimpiev, S.; Grechnikov, A.; Sunner, J.; Karavanskii, V.; Simanovsky, Y.; Zhabin, S.; Nikiforov, S. On the Role of Defects and Surface Chemistry for Surface-Assisted Laser Desorption Ionization from Silicon. *J. Chem. Phys.* **2008**, *128*, 014711.
(48) De Boor, J.; Kim, D. S.; Ao, X.; Hagen, D.; Cojocaru, A.; Föll, H.; Schmidt, V. Temperature and Structure Size Dependence of the Thermal Conductivity of Porous Silicon. *EPL (Europhys. Lett.* **2011**, *96*, 16001.
(49) Wang, Z.; Alaniz, J. E.; Jang, W.; Garay, J. E.; Dames, C. Thermal Conductivity of Nanocrystalline Silicon: Importance of Grain Size and Frequency-Dependent Mean Free Paths. *Nano Lett.* **2011**, *11*, 2206−2213.
(50) Shinoda, H.; Nakajima, T.; Ueno, K.; Koshida, N. Thermally Induced Ultrasonic Emission From Porous Silicon. *Nature* **1999**, *400*, 853−855.
(51) Amin-Chalhoub, E.; Semmar, N.; Coudron, L.; Gautier, G.; Boulmer-Leborgne, C.; Petit, A.; Gaillard, M.; Mathias, J.; Millon, E. Thermal Conductivity Measurement of Porous Silicon by the Pulsed-Photothermal Method. *J. Phys. D: Appl. Phys.* **2011**, *44*, 355401.
(52) Kovalev, D.; Polisski, G.; Ben-Chorin, M.; Diener, J.; Koch, F. The Temperature Dependence of the Absorption Coefficient of Porous Silicon. *J. Appl. Phys.* **1996**, *80*, 5978.
(53) Glassbrenner, C. J.; Slack, G. A. Thermal Conductivity of Silicon and Germanium from 3K to Melting Point. *Phys. Rev.* **1964**, *134*, A1058−A1069.
(54) Okhotin, A. S.; Pushkarskii, A. S.; Gorbachev, V. V. *Thermophysical Properties of Semiconductors*; Atom: Moscow, 1972.

DOI: 10.1021/jp5129063
J. Phys. Chem. C 2015, 119, 6382−6388